JOURNAL OF SOLID STATE CHEMISTRY 116, 61–67 (1995)

The Layered Composite Crystal Structure of the Ternary Sulfide $(BiS)_{1.11}NbS_2$

Y. Gotoh,[1] J. Akimoto, M. Goto, Y. Oosawa, and M. Onoda*

*National Institute of Materials and Chemical Research, Higashi, Tsukuba, Ibaraki 305, Japan; and *National Institute for Research in Inorganic Materials, Namiki, Tsukuba, Ibaraki 305, Japan*

Received May 26, 1994; accepted September 8, 1994

Single crystals of a new mutually incommensurate composite crystal with layered structure, $(BiS)_{1.11}NbS_2$ were synthesized and the average substructures were studied by the single crystal X-ray diffraction method. The commensurate superlattice reflections along mutually incommensurate directions were observed for the BiS subsystem with the main diffractions of the NbS_2 subsystem. The NbS_2 subsystem with a = 5.7504(9) Å, b_1 = 3.3306(11) Å, c = 23.0001(17) Å, Z = 4, and space group $F2mm$ takes the form of 2H-type NbS_2 sandwiches with Nb atoms trigonal-prismatically coordinated by S atoms. The BiS subsystem with a = 5.752(4) Å, b_2 = 36.156(5) Å, c = 23.001(5) Å, Z = 48, and space group $F2mm$ has distorted two-atom-thick double layers with an NaCl-type superstructure. The superstructure has Bi–Bi bonds and nonbonded S–S pairs along mutually incommensurate directions. The periodic length of b_2 is six times as large as those of simple NaCl-type arrangements. The Bi–Bi bonds are located in each half-length of b_2 in the BiS double layers. Each NbS_2 sandwich and BiS double layer stack alternately to form a mutually incommensurate composite crystal with a layered structure. The structural relations among $(BiX)_xTX_2$ (T = Nb, Ta; X = S, Se) type compounds are also discussed.

INTRODUCTION

Ternary chalcogenides with layered composite crystal structures $(MX)_xTX_2$ (M = Pb, Sn, rare earth elements; T = Ti, V, Nb, Ta, Cr; X = S, Se; x = 1.1–1.2) are composed of three-atom-thick TX_2 sandwiches and two-atom-thick MX double layers, alternately stacked. (1–21).

In the TX_2 sandwiches with T = Ti, V, and Cr, T atoms are octahedrally coordinated by X atoms, and 1T-type TX_2 sandwiches are formed. On the other hand, Nb and Ta are trigonal-prismatically coordinated by X atoms, and 2H-type TX_2 sandwiches are obtained.

The MX double layers between the TX_2 sandwiches generally have a distorted NaCl-type structure with M atoms protruding toward the pseudohexagonal planes of the X atoms of the TX_2 sandwiches.

[1] To whom correspondence should be addressed.

The TX_2 sandwiches and MX layers are incommensurate because the ratio of the in-plane lattice constants of the average structures of the two subsystems is irrational. As for the stacking direction of $(MX)_xTX_2$ compounds, lattice dimensions are equal or commensurate between the two subsystems. $(MX)_xTX_2$ compounds, therefore, form a quasiperiodic system which can be described with (3 + 1)-dimensional superspace group symmetry and are called composite crystals and/or misfit layered crystals with two interpenetrating subsystems (6, 11, 12, 16, 22–26, 28).

The stacking sequences of $(MX)_xTX_2$ compounds are simply explained based only on the two-dimensional commensurate section of $(MX)_xTX_2$ which is common to both subsystems. In this section, the protruded M atoms of the MX double layers are located at the dimple interposed by X atoms of the TX_2 sandwiches. For the compounds with 2H-type TX_2 sandwiches, in particular, four forms of the stacking model of $(MX)_xTX_2$ compounds with orthorhombic symmetry are thus proposed (5). Each subsystem in the orthorhombic compound is able to take a C-centered lattice with c in the range from about 11 to 12 Å or an F-centered one with c from about 22 to 24 Å. Consequently, four combinations of subsystems of C : C, C : F, F : C, and F : F types are possible.

Along the mutually incommensurate direction, (i.e., the direction in which the two layers are incommensurate), on the other hand, the quasiperiodic interactions between the TX_2 sandwiches and the MX double layers suggest that $(MX)_xTX_2$ compounds may be expected to show unique physical properties and crystal structures. Recently, the preparation and structure determination of single crystals of mutually commensurate $(BiSe)_{1.09}TaSe_2$ (27, 28) and mutually incommensurate $(BiS)_{1.07}TaS_2$ (29) compounds were reported. In these compounds, the TaX_2 sandwiches have a rather rigid 2H-type structure as do the TaX_2 ones in other $(MX)_xTaX_2$ compounds, while BiX double layers have a superstructure of the MX ones with a simple NaCl-type arrangement along the mutually commensurate or incommensurate directions. Both of the BiX double layers

0022-4596/95 $6.00

in $(BiSe)_{1.09}TaSe_2$ and $(BiS)_{1.07}TaS_2$ contain bond between the Bi atoms and not between the Se or S atoms in their superstructure. However, the quite different types of X-ray diffraction patterns observed for $(BiSe)_{1.09}TaSe_2$ and $(BiS)_{1.07}TaS_2$ have shown that the ordered structures with Bi–Bi bonds in both compounds are distinct from each other. In addition, the BiSe subsystem in $(BiSe)_{1.09}TaSe_2$ is mutually commensurate with the $TaSe_2$ subsystem, whereas the BiS subsystem in $(BiS)_{1.07}TaS_2$ is mutually incommensurate with the TaS_2 subsystem. These features described briefly above seem to allow further varieties of crystal structures in the series of $(BiX)_xTX_2$ type composite crystals.

In the present work, we have made single crystals of a new ternary sulfide, $(BiS)_{1.11}NbS_2$, and investigated its crystal structure. Furthermore, the crystal structure of $(BiS)_{1.11}NbS_2$ will be discussed in comparison with those of $(BiSe)_{1.09}TaSe_2$ and $(BiS)_{1.07}TaS_2$.

TABLE 1
Experimental Summary for $(BiS)_{1.11}NbS_2$

Subsystem	BiS	NbS_2
Crystal system	Orthorhombic	Orthorhombic
a (Å)	5.752(4)	5.7504(9)
b (Å)	36.156(5)	3.3306(11)
c (Å)	23.001(5)	23.0001(17)
Z	48	4
Diffractometer	Rigaku AFC-5	
Radiation (Å)	Mo$K\bar{\alpha}$ 0.71073	
θ range: min, max (°)	1.5, 35.0	1.5, 40.0
Scan mode	$2\theta - \omega$	$2\theta - \omega$
	$\Delta\omega = 1.50 + 0.35 \tan\theta$	$\Delta\omega = 1.30 + 0.35 \tan\theta$
Data set	h: 0–9, k: 0–58, l: 0–37	h: 0–10, k: 0–6, l: 0–41
Observed reflections with $\lvert F_o\rvert \geq 2.5\sigma(\lvert F_o\rvert)$	1933	407

EXPERIMENTAL

A powder sample was prepared using elements as starting material. The ratio of the elements was 1 : 1 : 3 for Bi, Nb, and S. The elements were heated at about 800°C in an evacuated quartz tube. Crystals were grown as thin platelets with a metallic luster from the powdered products using the chemical vapor transport method. The temperature gradient of the electric furnace used was controlled from 900 to 700°C and samples were maintained for about 1 week. About 15 mg of NH_4Cl used as the transfer reagent was added to the quartz tube with about 500 mg of powdered $(BiS)_{1.11}NbS_2$. A single crystal of $(BiS)_{1.11}NbS_2$ with dimensions about $0.4 \times 0.3 \times 0.02$ mm^3 was used for the structure analysis. A precession camera technique with Mo$K\bar{\alpha}$ radiation ($\lambda = 0.71073$ Å) was used to determine the crystal system and cell dimensions of each subsystem of $(BiS)_{1.11}NbS_2$. We have taken the b-axis as the mutually incommensurate direction as for the series of first structure determinations of $(LaS)_{1.20}CrS_2$ with triclinic symmetry (1, 6) and $(PbS)_{1.12}VS_2$ with monoclinic symmetry (9, 11). The X-ray reflection data of both subsystems were collected together with common $h0l$ reflections using a Rigaku AFC5 diffractometer (Mo$K\bar{\alpha}$ radiation). The cell parameters and data collection process are summarized in Table 1. The cell parameters were refined by a least-squares method using reflections in the range $20° < 2\theta < 30°$. The composition of $(BiS)_{1.11}NbS_2$ was determined from the ratio of cell dimensions of each subsystem. Lorentz polarization corrections and absorption corrections using the ψ-scan empirical method were applied to all of the collected reflections. All of the calculations for structure analysis were carried out using the UNICS III system (30). In all our calculations, neutral atomic scattering factors were taken from Cromer and Mann (31). Anomalous dispersion factors used throughout this procedure are those given by Cromer and Liberman (32).

RESULTS AND DISCUSSION

NbS_2 Subsystem

The X-ray precession photograph with the $hk0$ reflections of $(BiS)_{1.11}NbS_2$ showed the composite reflection patterns of the NbS_2 subsystem and the BiS subsystem. The schematic representation of each diffraction pattern is given in Fig. 1. Every diffraction observed is classified into two sets with an orthorhombic system, that is, $\{h\ k_1\ l\}$ for the NbS_2 subsystem and $\{h\ k_2\ l\}$ for the BiS subsystem.

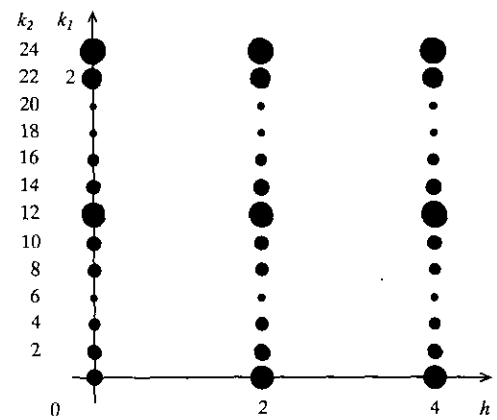

FIG. 1. Schematic representation of the X-ray diffraction pattern with $hk0$ type reflections of $(BiS)_{1.11}NbS_2$ observed by a precession photograph. The main reflections of the NbS_2 subsystem are indexed with k_1 and the superlattice reflections of the BiS subsystem are indexed with k_2. The reflections with $h00$ are common to both subsystems.

TABLE 2
Atomic Parameters and Equivalent Temperature Factors (Å^2) for the NbS_2 Subsystem (esd's in Parentheses)

	x	y	z	B_{eq}	Occupancy
Nb	0.0	0.0	0.0	0.2(3)	0.5
S	0.335(6)	0.0	0.0672(17)	0.5(9)	1.0

Note. $B_{eq} = (8\pi^2/3)\sum_i\sum_j U_{ij}a_i^*a_j^*a_i \cdot a_j$, where U_{ij} is the mean square displacement tensor of atoms.

The diffraction vector $\mathbf{q}$ of $(BiS)_{1.11}NbS_2$ is, therefore, expressed as

$$\mathbf{q} = ha^* + k_1b_1^* + lc^* + k_2b_2^*.$$

The reflections with k_1, $k_2 = 0$ are common to both subsystems.

The NbS_2 subsystem is present as the F-centered lattice defined by the orthorhombic space group $F2mm$ with $a = 5.7504(9)$ Å, $b_1 = 3.3306(11)$ Å, $c = 23.0001(17)$ Å. The structure model with two 2H-type NbS_2 sandwiches in the unit cell was adopted in the course of structural analysis. This model has been already recognized for other NbS_2 subsystems with orthorhombic symmetry in $(PbS)_{1.14}NbS_2$ (7), $(LaS)_{1.14}NbS_2$ (3, 7, 10, 12), $(CeS)_{1.16}NbS_2$ (14), $(SmS)_{1.19}NbS_2$ (15), and $(NdS)_{1.18}NbS_2$ (21) compounds. All of the parameters were refined by means of the full-matrix least-squares method, where the value of $R_w^2 = \Sigma\, w(|F_o| - |F_c|)^2/\Sigma\, w|F_o|^2$ was minimized. The final refinement converged with R-value of 0.116 and R_w-value ($w = 1/\sigma^2(F)$) of 0.149 using 310 reflections excluding the $h0l$ type. The atomic parameters of NbS_2 subsystem are listed in Table 2.

In the 2H-type NbS_2 sandwiches, Nb atoms as well as S atoms form pseudohexagonal planes and each Nb atom is trigonal-prismatically surrounded by six neighboring S atoms (Fig. 2). The value of the ratio a/b_1 is 1.7265, which is quite close to $\sqrt{3}$ for the hexagonal system. The Nb–Nb distances are 3.3227(4) Å (×4) and 3.3306(11) Å (×2). The Nb–S distances are 2.46(3) Å (×4) and 2.47(3) Å (×2). The thickness of each sandwich is 3.09(5) Å. Consequently, the NbS_2 sandwiches are less distorted than the BiS double layers which will be described below. It is concluded that the NbS_2 sandwiches have a fairly rigid 2H-type structure which can be regarded as the host part of $(BiS)_{1.11}NbS_2$ as in other $(MS)_xNbS_2$ compounds (3, 7, 10, 12, 14, 15, 21).

BiS Subsystem

The schematic representations of the X-ray diffraction patterns with $hk0$ reflections in Fig. 1 and $1kl$ reflections

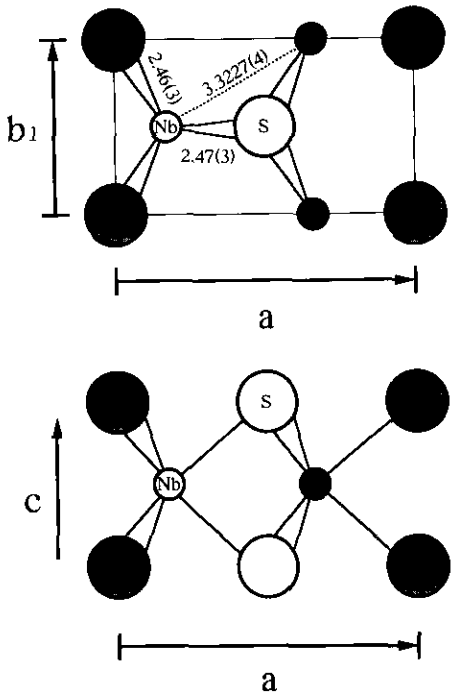

FIG. 2. The average structure of 2H-type NbS_2 sandwiches of the NbS_2 subsystem in $(BiS)_{1.11}NbS_2$.

in Fig. 3 suggest that the BiS subsystem in $(BiS)_{1.11}NbS_2$ has the NaCl-type superstructure along the mutually incommensurate b-axis. It is clearly shown that the intensities of the reflections with $k_2 = 0$, 12, 24 [$= 6(2n)$] are stronger than those with $k_2 = 2$, 10, 14, 22 [$= 6(2n) \pm 2$], $k_2 = 4$, 8, 16, 20 [$= 6(2n) \pm 4$], and $k_2 = 6$, 18 [$= 6(2n) \pm 6$] for hk_2l (h, $l = 2n$) (Fig. 1), and the reflections with $k_2 = 5$, 7, 17, 19 [$= 6(2n + 1) \pm 1$] are stronger than $k_2 = 3$, 9, 15, 21 [$= 6(2n + 1) \pm 3$] and $k_2 = 1$, 11, 13, 23 [$= 6(2n + 1) \pm 5$] for hk_2l (h, $l = 2n + 1$) (Fig. 3).

The diffraction patterns of the BiS subsystem in

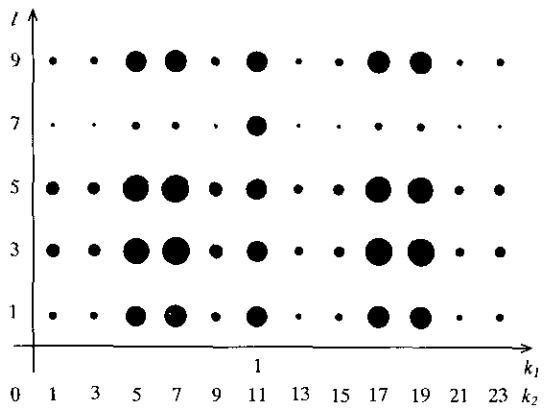

FIG. 3. Schematic representation of the X-ray precession photograph with $1kl$ type reflections of $(BiS)_{1.11}NbS_2$.

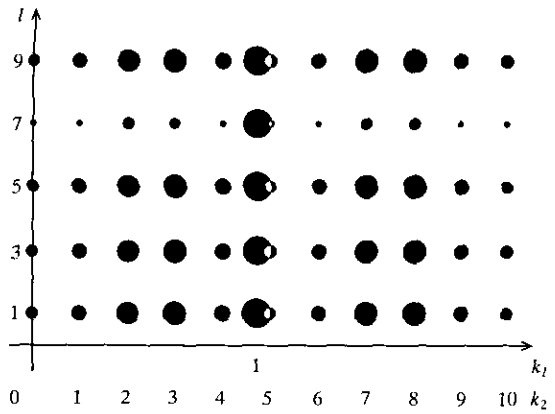

FIG. 4. Schematic representation of the X-ray precession photograph with $1kl$ type reflections of $(BiS)_{1.07}TaS_2$. The main reflections of the TaS_2 subsystem were indexed with k_1 and the superlattice reflections of the BiS subsystem were indexed with k_2.

$(BiS)_{1.11}NbS_2$ are similar to those reported for the BiSe subsystem defined by the orthorhombic space group $F2mm$ with $a = 5.967$ Å, $b_2 = 37.62$ Å, and $c = 24.342$ Å in $(BiSe)_{1.09}TaSe_2$ (27, 28). (To simplify the discussion, the lattice parameters of the BiSe subsystem presented here are given by interchanging the a-axis with the b-axis in the original form with $Fm2m$ symmetry.) They are, however, quite clearly distinguished from another type of superstructure pattern obtained for the BiS subsystem in $(BiS)_{1.07}TaS_2$ (29) (Fig. 4). As for the $(BiS)_{1.07}TaS_2$, the BiS subsystem is present as the B-centered lattice defined by the orthorhombic space group $B2mm$ with $a = 5.732(4)$ Å, $b_2 = 15.368(6)$ Å, $c = 23.135(5)$ Å. The schematic representation of the X-ray diffraction pattern of the BiS subsystem in $(BiS)_{1.07}TaS_2$ given in Fig. 4 shows that the reflections with $k_2 = 2, 3, 7, 8$ [$= \{5(2n + 1) \pm 1\}/2$] are stronger than those with $k_2 = 1, 4, 6, 9$ [$= \{5(2n + 1) \pm 3\}/2$] and $k_2 = 0, 5, 10$ [$= \{5(2n + 1) \pm 5\}/2$]. On the basis of the structure determinations, it has been found that these BiX (X = S, Se) subsystems with such characteristic patterns of intensities have Bi–Bi bonds and but no Se–Se or S–S bonds in their average substructure. The difference between these substructures is mainly the ordering of the Bi–Bi bonds.

For the structure analysis of the BiS subsystem in $(BiS)_{1.11}NbS_2$, we have, therefore, employed the superstructure model of the BiSe subsystem in $(BiSe)_{1.09}TaSe_2$ (27). All of the reflections are indexed with an F-centered superlattice as described above. The superstructure model with Bi–Bi bonds and no S–S bonds along the mutually incommensurate b-axis is defined by the orthorhombic space group $F2mm$ with $a = 5.752(4)$ Å, $b_2 = 36.156(5)$ Å, $c = 23.001(5)$ Å. In the structure model employed here, we must note that the simple NaCl-type arrangement of Bi and S atoms is retained along the a-axis which is common to the NbS_2 subsystem.

TABLE 3
Atomic Parameters and Equivalent Temperature Factors (Å^2) for the BiS Subsystem (esd's in Parentheses)

	x	y	z	B_{eq}	Occupancy
Bi(1)	0.0	0.0432(1)	0.3188(2)	1.3(1)	1.0
Bi(2)	−0.0012(11)	0.1243(1)	0.1799(2)	1.9(1)	1.0
Bi(3)	0.0226(8)	0.2087(1)	0.3173(1)	1.7(1)	1.0
S(1)	0.022(6)	0.0490(5)	0.1965(10)	1.5(5)	1.0
S(2)	0.028(6)	0.1337(6)	0.2962(10)	1.5(5)	1.0
S(3)	0.031(5)	0.2104(7)	0.2022(8)	1.7(4)	1.0

Note. $B_{eq} = (8\pi^2/3)\sum_i\sum_j U_{ij}a_i^*a_j^*a_i \cdot a_j$, where U_{ij} is the mean square displacement tensor of atoms.

The structure was refined using 823 reflections with $|F_o| \geq 6.0\sigma(|F_o|)$. The $h0l$ common reflections and $h\underline{11}l$, $h\underline{22}l$, $h\underline{33}l$, $h\underline{44}l$, and $h\underline{55}l$, ones that partially overlapped the main reflections of the NbS_2 subsystem were excluded throughout the calculations. In the structure refinement, the block-diagonal matrix least-squares method was used to avoid correlation between structural parameters. The refined atomic parameters are listed in Table 3, where the R-value converged to 0.083 and the R_w-value ($w = 1$) was 0.104. The list of selected atomic distances in a BiS double layer is given in Table 4. Along the common a-axis, the BiS double layers with simple NaCl-type arrangement are distorted in the same manner as the MS subsystems in other $(MS)_xNbS_2$ compounds (M = Pb, Sn and rare earth

TABLE 4
Selected Atomic Distances (Å) for the BiS Subsystem in $(BiS)_{1.11}NbS_2$ (esd's in Parentheses)

Bi(1)–S(1)	Bi(1)–S(1)	2.822(23)
	Bi(1)–S(1)^{ii}	2.78(3)
	Bi(1)–S(1)^{iii}	3.03(3)
Bi(1)–Bi(1)	Bi(1)–Bi(1)^{i}	3.125(3)
Bi(1)–S(2)	Bi(1)–S(2)	3.315(20)
S(1)–S(1)	S(1)–S(1)^{i}	3.545(27)
Bi(2)–S(1)	Bi(2)–S(1)	2.751(20)
Bi(2)–S(2)	Bi(2)–S(2)	2.701(22)
	Bi(2)–S(2)^{ii}	3.11(3)
	Bi(2)–S(2)^{iii}	2.79(3)
Bi(2)–S(3)	Bi(2)–S(3)	3.160(27)
Bi(3)–S(2)	Bi(3)–S(2)	2.755(20)
Bi(3)–S(3)	Bi(3)–S(3)	2.647(19)
	Bi(3)–S(3)^{ii}	2.86(3)
	Bi(3)–S(3)^{iii}	2.96(3)
	Bi(3)–S(3)^{iv}	2.961(27)

Note. Symmetry operations: (i) $x, -y, z$; (ii) $x + 1/2, y, -z + 1/2$; (iii) $x - 1/2, y, -z + 1/2$; (iv) $x, -y + 1/2, -z + 1/2$.

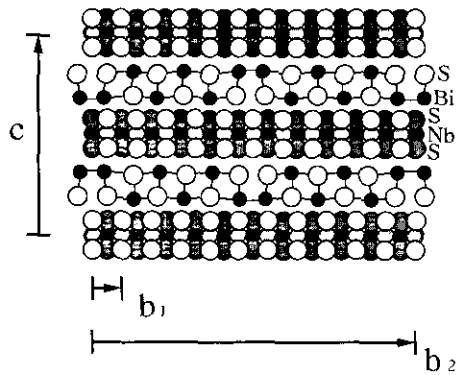

FIG. 5. Projection of the average structure of $(BiS)_{1.11}NbS_2$ along the common a-axis.

elements) (3, 7, 10, 12 14, 15, 21). That is, all Bi atoms protrude toward the NbS_2 sandwiches. The distorted BiS double layers and the rather rigid NbS_2 sandwiches will be related to each other with a two-dimensional commensurate section using the common $h0l$ reflections.

The short Bi–Bi bonds appear in every $b_2/2$, that is, every half of the cell dimension along the mutually incommensurate b-axis (Fig. 5). Antiphase domain boundaries across the Bi–Bi bonds and nonbonded S–S pairs are simultaneously present along the b-direction. In each domain, a distortion of Bi and S atoms similar to that observed along the common a-axis occurs, which is also recognized for $(BiSe)_{1.09}TaSe_2$ (27, 28), and $(BiS)_{1.07}TaS_2$ (29). The short calculated Bi–Bi distance is 3.125(3) Å, which is almost the same value as 3.109 Å for the BiSe subsystem in $(BiSe)_{1.09}TaSe_2$ (28) and 3.120 Å for the BiS one in $(BiS)_{1.07}TaS_2$ (29). As for the BiS subsystem in $(BiS)_{1.07}TaS_2$, short Bi–Bi bonds are present in every supercell, which is 2.5 times as large as the unit cell of the simple NaCl-type MS subsystem in other $(MS)_xTaS_2$ compounds (Fig. 6). Both of the BiSe subsystem in $(BiSe)_{1.09}TaSe_2$ and the BiS subsystem in $(BiS)_{1.11}NbS_2$

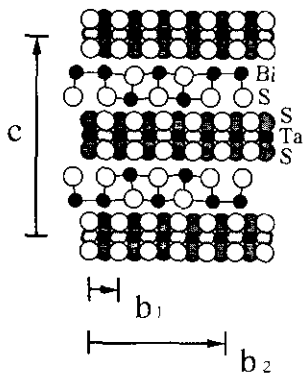

FIG. 6. Projection of the average structure of $(BiS)_{1.07}TaS_2$ along the common a-axis.

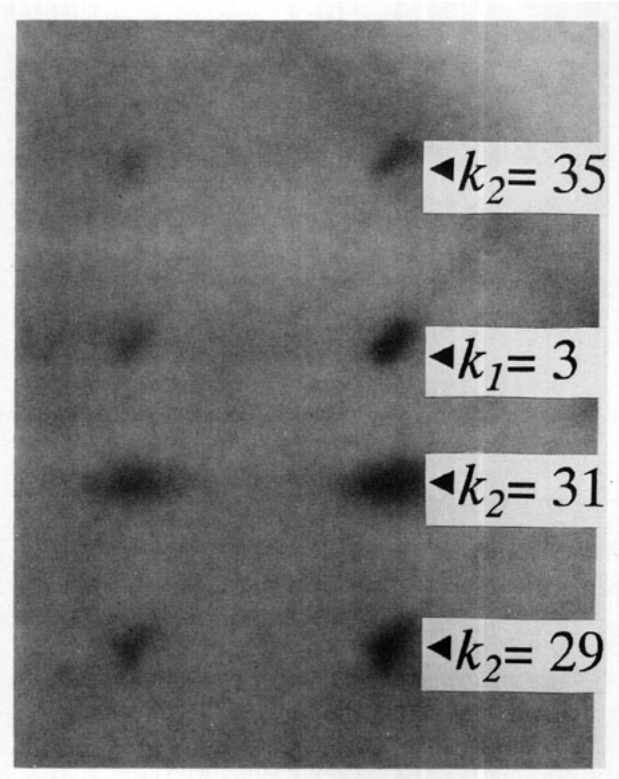

FIG. 7. Precession photograph with $1kl$ reflections of $(BiS)_{1.11}NbS_2$, where only the region with high values of k_1 and k_2 is partially magnified.

have supercells with b_2 six times as long as the unit cell of the simple NaCl-type subsystem.

In $(BiSe)_{1.09}TaSe_2$, the BiSe subsystem with a = 5.967 Å, b_2 = 37.62 Å, and c = 24.342 Å is mutually commensurate with the $TaSe_2$ subsystem with a = 5.970 Å, b_1 = 3.421 Å, and c = 24.341 Å (28). The b_2 value of the supercell of the BiSe subsystem is 11 times as large as the b_1 value of the $TaSe_2$ subsystem. However, the BiS subsystem is mutually incommensurate with the NbS_2 subsystem in $(BiS)_{1.11}NbS_2$ (Fig. 5). Though the reflections with k_1 = 1 for the NbS_2 subsystem and k_2 = 11 for the BiS subsystem are almost indistinguishable, the reflections with k_1 = 3 are present at the positions clearly displaced from those expected for ones with k_2 = 33 (Fig. 7). The intensities of the reflections with k_2 = 33 were too weak to be observed in our present measurement. The deviation from the commensurate ratio of 1/11 is calculated to be $(b_1/b_2 - 1/11) \approx 0.0012$, which is significantly larger than the corresponding value of 0.00003 obtained for the mutually commensurate $(BiSe)_{1.09}TaSe_2$ (28). The BiS subsystem in $(BiS)_{1.07}TaS_2$ which has another type of superstructure is also mutually incommensurate with the TaS_2 subsystem with 2H-type sandwiches (Fig. 6). In $(BiS)_{1.07}TaS_2$, the reflections with k_1 = 1 for the TaS_2 subsystem and the reflections with k_2 = 5 for

TABLE 5
Atomic Parameters and Isotropic Temperature Factors (Å^2) for $(BiS)_{1.11}NbS_2$ along the *b*-Axis (esd's in Parentheses)

	x	*y*	*z*	B_{iso}	Occupancy
Bi	0.5990(15)	—	0.1822(5)	1.0(2)	0.5528
S	0.042(5)	—	0.1841(29)	0.2(7)	0.5528
Nb	0.0	—	0.0	0.5(3)	0.5
S	0.330(4)	—	0.0687(14)	0.2(4)	1.0

the BiS subsystem are quite explicitly separated from each other (Fig. 4).

Commensurate Section

The common *h0l* reflections were essential to show that $(BiS)_{1.11}NbS_2$ is a composite crystal with two interpenetrating subsystems. The commensurate section of $(BiS)_{1.11}NbS_2$ was defined by the space group *B2mm* with $a = 5.7504(9)$ Å and $c = 23.0001(17)$ Å. The refinement converged to an *R*-value of 0.136 and an R_w-value ($w = 1/\sigma^2(F)$) of 0.152 using 76 reflections. The corresponding atomic parameters are listed in Table 5. The occupancy for the BiS subsystem, calculated using the value of b_1, b_2, and *Z* in Table 1 as $(48b_1/4b_2)/2 = 0.5528$, was fixed in the refinement.

The arrangements of Bi and S atoms obtained in the BiS double layers are simple NaCl-type along the common *a*-axis. In the *ac*-commensurate section given in Fig. 8, the BiS double layers are distorted and the protruded Bi atoms preferably fall into the dimples of the planes of the S atoms in the 2H-type NbS_2 sandwiches with a much more undistorted structure.

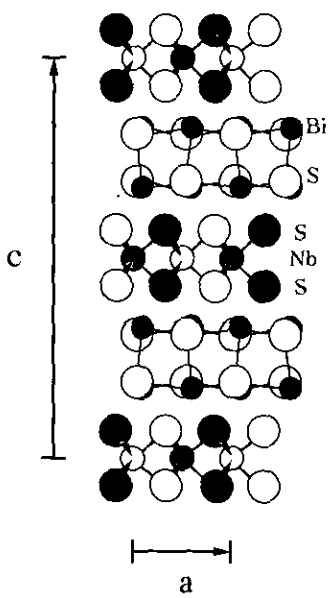

FIG. 8. Projection of the common section of $(BiS)_{1.11}NbS_2$ along the mutually incommensurate direction.

The distortion of the *MX* double layers (*M* = Pb, Sn, rare earth elements, Bi) between every two 2H-type NbX_2 or TaX_2 (*X* = S, Se) sandwiches seems to be essential in stabilizing the ordering of the alternate stacking sequences in all of the $(MX)_xNbX_2$ and $(MX)_xTaX_2$ compounds. In the same manner, we can further understand the presence of triclinic $(LaS)_{1.20}CrS_2$ with 1T-type CrS_2 sandwiches and monoclinic $(PbS)_{1.12}VS_2$ with 1T-type VS_2 ones, though binary CrS_2 and VS_2 are respectively known to be unstable and metastable compounds. From the studies of their structure determination (1, 6, 9, 11), both of the LaS and the PbS double layers between these 1T-type sandwiches have the distorted NaCl-type structure, and La and Pb atoms also protrude toward the dimple of the planes of S atoms of the CrS_2 and/or the VS_2 sandwiches.

CONCLUSION

In the present study, we have prepared the single crystal of $(BiS)_{1.11}NbS_2$, a composite crystal with mutually incommensurate layers. Both of the average substructures were determined together with a commensurate structure with two interpenetrating subsystems. The NbS_2 subsystem has 2H-type three-atom-thick sandwiches with a rather rigid structure. The BiS subsystem has double layers with the NaCl-type superstructure along the mutually incommensurate direction. In the superstructure, bonded Bi–Bi and nonbonded S–S pairs are located in the same manner as found in the superstructure of the BiSe subsystem in mutually commensurate $(BiSe)_{1.09}TaSe_2$. We have also compared the structure of the mutually incommensurate $(BiS)_{1.11}NbS_2$ with those of the mutually commensurate $(BiSe)_{1.09}TaSe_2$ and another type of mutually incommensurate $(BiS)_{1.07}TaS_2$.

REFERENCES

1. K. Kato, I. Kawada, and T. Takahashi, *Acta Crystallogr. Sect. B* **33,** 3437 (1977).
2. G. A. Wiegers, A. Meetsma, R. J. Haange, and J. L. de Boer, *Mater. Res. Bull.* **23,** 1551 (1988).
3. A. Meerschaut, P. Rabu, and J. Rouxel, *J. Solid State Chem.* **78,** 35 (1989).
4. A. Meetsma, G. A. Wiegers, R. J. Haange, and J. L. de Boer, *Acta Crystallogr. Sect. A* **45,** 285 (1989).
5. G. A. Wiegers, A. Meetsma, S. van Smaalen, R. J. Haange, J. Wulff, T. Zeinstra, J. L. de Boer, S. Kuypers, G. van Tendeloo, J. van Landuyt, S. Amelinckx, A. Meerschaut, P. Rabu, and J. Rouxel, *Solid State Commun.* **70,** 409 (1989).
6. K. Kato, *Acta Crystallogr. Sect. B* **46,** 39 (1990).
7. G. A. Wiegers, A. Meetsma, R. J. Haange, S. van Smaalen, J. L. de Boer, A. Meerschaut, P. Rabu, and J. Rouxel, *Acta Crystallogr. Sect. B* **46,** 324 (1990).

8. J. Wulff, A. Meetsma, S. van Smaalen, R. J. Haange, J. L. de Boer, and G. A. Wiegers, *J. Solid State Chem.* **84,** 118 (1990).
9. Y. Gotoh, M. Goto, K. Kawaguchi, Y. Oosawa, and M. Onoda, *Mater. Res. Bull.* **25,** 307 (1990).
10. A. Meerschaut, P. Rabu, J. Rouxel, P. Monceau, and A. Smontara, *Mater. Res. Bull.* **25,** 855 (1990).
11. M. Onoda, K. Kato, Y. Gotoh, and Y. Oosawa, *Acta Crystallogr. Sect. B* **46,** 487 (1990).
12. S. van Smaalen, *J. Phys. Condens. Matter* **3,** 1247 (1990).
13. P. Rabu, A. Meerschaut, J. Rouxel, and G. A. Wiegers, *J. Solid State Chem.* **88,** 451 (1990).
14. G. A. Wiegers, A. Meetsma, R. J. Haange, and J. L. de Boer, *J. Solid State Chem.* **89,** 328 (1990).
15. A. Meerschaut, C. Auriel, A. Lafond, C. Deudon, P. Gressier, and J. Rouxel, *Eur. J. Solid State Inorg. Chem.* **28,** 581 (1991).
16. S. van Smaalen, A. Meetsma, G. A. Wiegers, and J. L. de Boer, *Acta Crystallogr. Sect. B* **47,** 314 (1991).
17. J. L. de Boer, A. Meetsma, Th. J. Zeinstra, R. J. Haange, and G A. Wiegers, *Acta Crystallogr. Sect. C* **47,** 924 (1991).
18. G. A. Wiegers, A. Meetsma, J. L. de Boer, S. van Smmalen, and R. J. Haange, *J. Phys. Condens. Matter* **3,** 2603 (1991).
19. G. A. Wiegers, A. Meetsma, R. J. Haange, and J. L. de Boer, *J. Less-Common Met.* **168,** 347 (1991).
20. G. A. Wiegers and A. Meerschaut, *J. Alloys Compounds* **178,** 351 (1992).
21. A. Lafond, A. Meerschaut, P. Gressier, and J. Rouxel, *J. Solid State Chem.* **103,** 458 (1993).
22. A. Janner and T. Janssen, *Acta Crystallogr. Sect. A* **36,** 408 (1980).
23. T. Janssen, *Acta Crystallogr. Sect. A* **47,** 243 (1991).
24. S. van Smmalen, *Phys. Rev. B* **43,** 11,330 (1991).
25. A. Yamamoto, *Acta Crystallogr. Sect. A* **48,** 476 (1992).
26. A. Yamamoto, *Acta Crystallogr. Sect. A* **49,** 831 (1993).
27. W. Y. Zhou, A. Meetsma, J. L. de Boer, and G. A. Wiegers, *Mater. Res. Bull.* **27,** 563 (1992).
28. V. Petricek, I. Cisarova, J. L. de Boer, W. Zhou, A. Meetsma, G. A. Wiegers, and S. van Smaalen, *Acta Crystallogr. Sect. B* **49,** 258 (1993).
29. Y. Gotoh, M. Onoda, J. Akimoto, M. Goto, and Y. Oosawa, *Jpn. J. Appl. Phys.* **31,** 3946 (1992).
30. T. Sakurai and K. Kobayashi, *Rep. Inst. Phys. and Chem. Res.* **55,** 69 (1979).
31. D. T. Cromer and J. B. Mann, *Acta Crystallogr. Sect. A* **24,** 321 (1968).
32. D. T. Cromer and D. Liberman, *J. Chem. Phys.* **53,** 1891 (1970).